Investigation of historical severe storms and storm tides in the German Bight with century reanalysis data

Elke M. I. Meyer[1], Lidia Gaslikova[1]

[1]Helmholtz-Zentrum Hereon, Institute of Coastal Systems, Geesthacht, 21502, Germany

5

Correspondence to: Elke M. I. Meyer (elke.meyer@hereon.de)

Abstract

Century reanalysis models offer a possibility to investigate extreme events and gain further insights into their impact through numerical experiments. This paper is a comprehensive summary of historical hazardous storm tides in the German Bight
10 (southern North Sea) with the aim to compare and evaluate the potential of different century reanalyses data to be used for the reconstruction of extreme water levels. The composite analysis of historical water level extremes, underlying atmospheric situations and their uncertainties may further support decision making in coastal protection and risk assessment. The analysis is done based on the results of the regional hydrodynamic model simulations forced by atmospheric century reanalysis data, e.g., 20CR ensembles, ERA5 and UERRA-HARMONIE. The selected eight historical storms lead either to highest storm tide
15 extremes for at least one of three locations around the German Bight, or to extreme storm surge events during low tide. In general, extreme storm tides could be reproduced and some individual ensemble members are suitable for reconstruction of respective storm tides. However, the highest observed water level in the German Bight could not be simulated with any considered forcing. The particular weather situations with corresponding storm tracks are analysed to better understand their different impact on the peak storm tides, their variability and predictability. Storms with more northerly tracks generally show
20 less variability in wind speed and a better agreement with the observed extreme water levels for the German Bight. The impact of two severe historical storms that peaked at low tide is investigated with shifted tides. For Husum in the eastern German Bight this results in substantial increase of the peak water levels reaching historical maximum.

1 Introduction

The German Bight (Fig.1) as part of the south-eastern North Sea is exposed to storm tides, which represent natural hazards for
25 the low-lying coastal areas. In the last 120 years, a few severe storms occurred with partly considerable damages at the coasts of the German Bight and in the hinterland connected to the North Sea by the rivers (e.g., Ems, Weser, Elbe, Eider). One example is the storm on 16/17 February 1962 which has caused extensive damage due to very high water levels in the German Bight and insufficient protection at the coast and along the rivers. After this event, coastal defences have been significantly improved (e.g., higher dike line and barriers) and the storm tide on 03 January 1976, also one of the highest during the last 120
30 years, has caused lesser damage mainly due to the improved protection (Kuratorium für Forschung im Küsteningenieurwesen, 1979).

Despite the extensive improvement of coastal protection along the coasts of the German Bight risk of flooding is still present and will increase in the future in the context of anthropogenic climate change. The observational data of water level from the tide gauges extend more than a century back in time and provide an indispensable source of information about extreme storm
35 events and their impact on the coast. However, these measurements are sporadic by nature and for large parts of the coastline not available. The hydrodynamic models are traditionally used as an additional tool to estimate water levels along the coastline regularly. Storm tides, casing the main flooding hazard at the coasts, can be considered as a composition of atmospherically driven components like storm surge and external surge, tidal component, and their non-linear interaction. Leaving aside the

changing bathymetry, coastal outline and protection constructions, the main uncertainty in the modelling of historical storm tides originates in atmospheric forcing. Thus, the realistic reconstruction of wind and pressure fields during the storm is necessary for adequate storm tide estimations. As the observational atmospheric data over the sea are sparse and irregular, especially during the pre-satellite era, atmospheric reanalysis has appeared in the past three decades (e.g., NCEP-NCAR, ERA-40, ERA-Interim, ERA-20C, CERRA). These reconstructions of the atmospheric state are produced with atmospheric models, which also consider available measurements by assimilation procedure.

In recent years, more reanalysis products became available at higher spatial and temporal resolution, improving the representation of localised effects by resolving relevant mesoscale processes (e.g., ERA5 (Hersbach et al., 2020), UERRA-HARMONIE (Ridal et al., 2018, Schimanke et al., 2020)). These reanalyses provide atmospheric conditions for the more recent storms from 1950 onwards. However, events that occurred further back and are still relevant for design purposes are not included. Another type of reanalysis products, which also recently emerged, are the century reanalyses ensembles, e.g., Twentieth Century Reanalysis project (20CR), (Compo et al., 2011; Slivinski et al., 2019, 2021). These reanalyses are generated using a weather model, with measurements assimilated. They provide a set of physically consistent atmospheric conditions, which slightly differ due to internal variability in the system. The advantage of the ensemble is that it enables the estimation of uncertainties due to internal variability. Using this as an atmospheric forcing for a hydrodynamic model, it can help to answer the question of what the extreme storm tides would look like if the historical low-pressure areas developed slightly differently, and thus estimate the uncertainty not only due to variability but also due to imperfectly reconstructed historical conditions.

Another benefit of the 20CR reanalysis is that it goes further back in time, starting from 1836 or even 1806 with an experimental product. Hence, earlier historical storms can be reconstructed than it was possible with other reanalysis products (e.g., see Meyer et al. 2022 for the reconstruction of the 1906 storm). The longer period and multiple realisations of the reanalysis are somewhat counterbalanced by a coarser resolution (1° or 2°) and even sparser data used for assimilation. The reanalysis products use mainly observed atmospheric pressure data, which are constant in their measurement method and independent in their environment but limited in earlier years and over the ocean. Both factors can influence the storm tide reconstructions driven by these reanalyses.

For the North Sea region in particular, various combinations of atmospheric reanalyses and regional hydrodynamic models have been used and proved to be valid and effective tools for different water level related studies and applications. For example, Weisse and Plüß (2006) investigated the changes and multi-decadal variability of local extreme water levels using a hydrodynamic hindcast forced by NCEP-NCAR reanalysis refined with the SN-REMO regional model. Later, Weisse et al. (2015) applied a different hydrodynamic model and an improved regionalisation of NCEP-NCAR reanalysis to obtain a 67-year water level hindcast dataset used in several coastal and offshore applications. Arns et al. (2015a) and Arns et al. (2015b) used yet another hydrodynamic model forced by mean sea level pressure fields, u and v components of the 10 m wind fields of 20CR version 2 reanalysis for 40 years to investigate return water levels and influence of historical sea level rise on storm surge water levels in the German Bight. Vousdoukas et al. (2016) used the ERA-Interim driven hydrodynamic hindcast mainly for validation purposes for the European coasts. While these and other analogous studies nicely demonstrated the applicability of atmospheric reanalysis, they mostly focused on statistics and the long-term evolution of extreme events rather than on the representation and investigation of multiple separate historical events.

Coastal adaptation measures are usually a long-term and costly effort and a good knowledge of the prevailing environmental conditions and factors contributing to each storm event are important. Among others, some specific studies focused on individual storm events rather than on the statistical properties of extreme storm tides were performed to provide such information. Such studies are, for example, the research projects MUSE, XtremRisk and EXTREMENESS. Therein, either historical storm tides or storm tides from future climate projections were investigated. In particular, the question of whether the extreme historical storm tides could potentially be exceeded was tackled. In the research project MUSE (Model-based

investigations of storm surges with very low probabilities of occurrence on the North Sea coast, Jensen et al., 2006, Bork and Müller-Navarra, 2006) several historical storm tides were investigated. A forecast model was used to create an ensemble of physically possible wind and pressure situations that can cause exceptionally high storm tides. Observed and modelled water levels were statistically analysed to calculate highest water levels at the North Sea coasts. The project XtremRisk (Oumeraci et al., 2015; Gönnert and Gerkensmeier, 2015) combined results derived from observations of different storm surge components such as storm surge, external surge, tides and their non-linear interactions including future scenarios with sea-level rise. This project focused mainly on the eastern German Bight and the Elbe estuary in constructing physically possible extreme storm tides. In the project EXTREMENESS, a substantial number of datasets containing reanalyses, hindcasts and climate change projections were analysed to find highly unlikely but potentially possible storm events with high-risk potential at the southern German Bight. The highest selected events were simulated with different phase lags between the astronomical tides given at the lateral boundaries of the shelf and the wind forcing to analyse if the respective event could become higher (Ganske et al., 2018, Grabemann et al., 2020).

In the present study, we want to further explore historical storm tide events with the help of multiple available atmospheric reanalyses and address the following questions:

(a) Are the (century) reanalysis data suitable for simulation of historical strong and severe storm tide events, especially in the earlier period?

(b) How much variability exists in the atmospheric forcing and how the resulting uncertainty would influence the hazards associated with the extreme storm tides?

(c) What influence does the track position of low-pressure systems have on the water levels in the German Bight?

(d) Is there a potential for further amplification of extreme historical storm tides, for example, by coincidence with the astronomical high tide?

The paper is structured as follows: in Section 2, there is a brief overview of the historic severe storm tide events in the German Bight (2.1), and a description of the used reanalysis data (2.2), the hydrodynamic model and tides (2.3). In Section 3 the results are presented and discussed, and Section 4 follows with the conclusions.

2 Data and methods

2.1 Historical severe storm tide events

The impact of specific storms and storm tides in the North Sea and the German Bight varies along the coastal strips. For example, the storm tide on 03 Jan 1976 affected mainly the eastern parts of the German Bight and the Elbe estuary. The storm tides caused by the 1962 storm belong to the highest events along the entire German North Sea coast and the neighbouring countries. One of the highest observed water levels at the southern German Bight coast occurred during the 13 March 1906 event (van Bebber, 1906 and Deutsches Gewässerkundliches Jahrbuch (DGJ), 2014).

We selected three locations (Norderney, Cuxhaven and Husum) as representatives for the various coastal strips of the German Bight (Figure 1) and listed for each one the three highest water level events that occurred during the past century (DGJ, 2014). Additionally, their classification according to the Federal Maritime and Hydrographic Agency (Bundesamt für Seeschifffahrt und Hydrographie, BSH) is depicted. The classification of storm tide events depends on the average tidal magnitude at the location and exact thresholds for particular locations are listed in Table 1. The BSH defines water levels higher than 1.5m above mean high water (MHW) as storm tide, a severe storm tide is defined by water levels between 2.5 and 3.5m above mean high water. All water levels higher than 3.5m above MHW are defined as a very severe storm tide. This classification is valid for the Elbe estuary and the eastern German Bight. In the southern German Bight, even lower water levels cause major damage at the coast. In this region, the German DIN 4049-3 (Deutsches Institut für Normung e.V., 1994) classification is also applied.

A storm tide is defined as an event, which occurs 10 to 0.5 per year; a severe storm tide 0.5 to 0.05 per year and a very severe storm tide every twenty years. For Norderney, the water levels estimated for the period 1951-2010 are considered storm tide

125   if they exceed 0.93m, severe storm tide threshold is 2.01m and very severe storm tide is over 2.75 m (Streicher et al., 2015). These values are lower than the thresholds from the BSH definition (Table 1).

Classification	Definition	Norderney (MHW = 1.14m NAP)	Cuxhaven (MHW =1.46m NAP)	Husum (MHW = 1.58m NAP)
storm tide	more than 1.5 m above mean high tide (MHW)	2.64m	2.96m	3.08m
severe storm tide	more than 2.5 m above mean high tide	3.64m	3.96m	4.08m
very severe storm tide	more than 3.5 m above mean high tide	4.64m	4.96m	5.08m

Table 1: Storm tide definition by the BSH. MHW is calculated for the period 1961-1990 (https://stormsurge-monitor.eu,
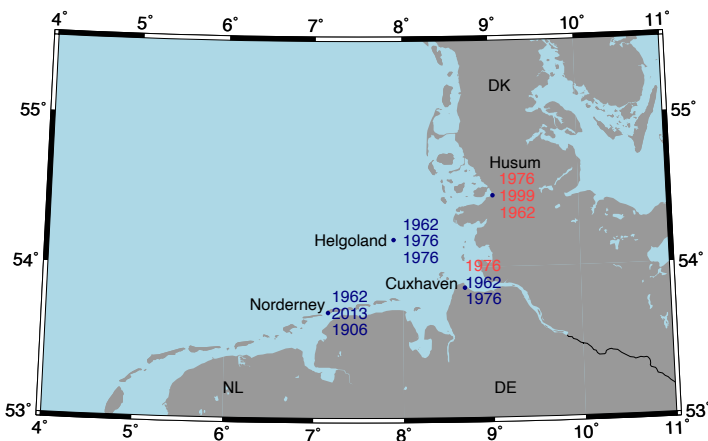130   2023); (Normaal Amsterdams Peil, NAP)

Figure 1: Three highest water level events observed since the beginning of regular observation at selected locations in the German Bight and their classification by the BSH (Table 1) in severe (blue) and very severe (red) storm tides.

135   The risk potential of individual storms and storm tides changes along the German North Sea coasts depending on the specific storm tracks and associated wind directions and wind set-up. The tracks of storms, which caused the most severe storm tides at one or another substantial region of the German Bight coasts, are shown in Figure 2; their description is complemented in Table 2. The tracks follow the minimum of the low-pressure area for each storm event with the sea-level pressure data derived from the ERA5 reanalysis starting from 1940. Several storm classification methods according to their tracks were proposed
140   and discussed in the literature in the past decades (e.g., Kruhl, 1978, Gerber et al., 2016 or Prügel, 1941; Schelling, 1952; Petersen and Rhode, 1991). Summarising, the typical storms associated with the storm tide hazard in the German Bight can be separated into the North-West (or Scandinavia) type and the West and South-West (or Jutland) type. In particular, Prügel (1941) defined the types according to the latitude at which they crossed the longitude 8°E (see Figure 2):

   -    Jutland type: 55° - 57°N
145   -   Skagerrak type: 57° - 60°N
   -    Scandinavia type: 60° - 65°N.

The East Frisian coasts (southern German Bight) have higher water level risks during storms travelling more in the north of Europe. Such storms are labelled as Scandinavia type and are characterized by a long fetch over the North Sea area and high surge in the entire southern North Sea, e.g., storm tide in 1962 (Rodewald, 1962, Koopmann, 1962 and Gönnert, 2003). The low-pressure system over Scandinavia and at the same time a high-pressure system in the Bay of Biscay generate high-pressure gradients and wind speed over the North Sea (Figure A1, a-c).

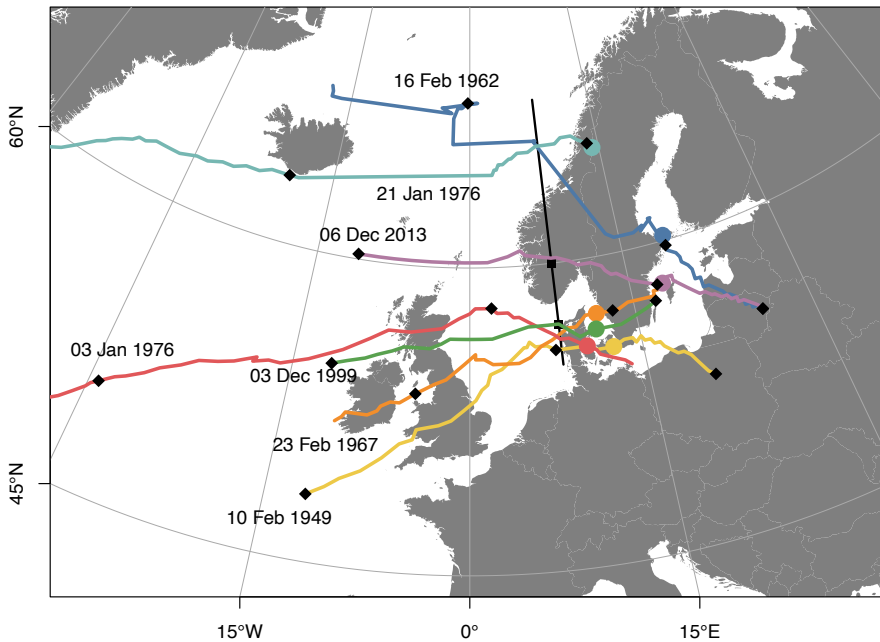## Storm tracks based on ERA5 data

Figure 2: Storm tracks derived from ERA5 data. Black diamonds mark midnight on the track. The coloured circles mark a specific date when the observed water level in Cuxhaven was highest during this event. The black line depicts longitude 8°E as the basis for the storm tide classification according to Prügel (1941). The squares separate the types in Jutland, Skagerrak, and Scandinavia type. For additional information about mean sea-level pressure during the single events, see Figure A1.

Date of event	Type (Kruhl, 1978)	Type (Prügel, 1942)
13 Mar 1906	West and South-West Type	Skagerrak Type
10 Feb 1949	West and South-West Type	Jutland Type
16 Feb 1962	North-West Type	Scandinavia Type
23 Feb 1967	West and South-West Type	Jutland Type
03 Jan 1976	West and South-West Type	Jutland Type
21 Jan 1976	North-West Type	Scandinavia Type
03 Dec 1999	West and South-West Type	Jutland Type
06 Dec 2013	North-West Type	Scandinavia Type

Table 2: In this study, a selection of severe storms and storm tides in the German Bight is investigated. See also Figure 1.

Fast-moving storms with more southerly tracks, so called Jutland type, are characterized by high wind speeds and steep wind surge at the eastern German Bight, e.g., the storm on 3rd December 1999. The Elbe estuary is situated between the two regions and storms of both types were able to cause some of the most extreme observed water levels there. The highest observed storm tide at Cuxhaven during the storm on 3rd January 1976 was induced by a storm of the Jutland type (Figure A1, d). The situation was exacerbated by the timing of the tide. Namely, the wind speed peak at the Elbe mouth co-occurred with low tide, thus

5

preventing the tide propagated earlier upstream the river from being released back to the North Sea, which led to an additional water level increase on top of the wind surge. The second highest storm tide in the Elbe estuary was caused by a storm of the Scandinavian type in 1962, which had a prominent impact on the entire German Bight.

Due to partly stochastic nature of maximum storm surge and tidal high water coincidence (e.g. discussion in Horsburgh and Wilson, 2007), some extreme storm surges did not result in extreme storm tides at the coast. Still, such events are of interest because they present the atmospheric conditions, which may lead to extreme water levels when coincide with high tide. So, Figure 2 shows additionally the tracks of two storm events, which caused extreme surges during low tide and therefore did not lead to very high water levels. The first one, on 10 Feb. 1949 is known for the highest observed surge in Husum and the second one, on 23 Feb. 1967, for the highest observed wind speeds on Helgoland (Tomczak,1950, Lamb, 2005).

2.2 Atmospheric reanalysis products

The basis for this study is the century reanalysis data, in particular the products from the 20th Century Project (20CRv2c and 20CRv3) (Compo et al., 2011; Slivinski et al., 2019, 2021). This is an ensemble of global forecast model results with assimilated observations, e.g., pressure data from the International Surface Pressure Databank (ISPD). Observed pressure data have a long history and are robust concerning systematic measurement errors (Schmidt and von Storch, 1993; Alexandersson et al., 1998, 2000). Thus, the reanalysis dataset represents atmospheric conditions consistent with available observations but slightly varying due to internal variability, especially in the regions with lacking measurement data. In total, 56 members for 20CRv2c and 80 members for 20CRv3 were used. Additionally, to the ensemble reanalyses, the results from the ECMWF (European Centre for Medium-Range Weather Forecasts) ERA5 and UERRA-HARMONIE, in the following UERRA, reanalysis were used (Hersbach et al., 2018, Ridal et al., 2018, UERRA). These data have higher spatial and temporal resolution, which may have an impact on the quality of the extreme water level simulations. As an additional refinement, the UERRA data were merged with OptempS data (Kristandt et al., 2014). In the OptempS project, high-resolution data in time and space were produced with a German forecast model to get more precise atmospheric conditions for the reconstruction of storm surges. Forty events starting from 1960 were reanalysed in the project with ERA-40 (Uppala, et al., 2005) and ERA-Interim (Dee et al.,2011) data used as initial conditions (Kristandt et al., 2014). The OptempS data are available approximately three days before and two days after the storm event. The main features of each used dataset are summarised in Table 3.

Reanalysis	Short form	Number of used ensemble members	Starting year	Spatial resolution	Temporal resolution
20th Century Reanalysis Project version 2c	20CRv2c	56	1851	2° x 2°	6-/3-hourly
20th Century Reanalysis Project version 3	20CRv3	80	1836	1° x 1°	3-hourly
ECMWF ERA5	ERA5	1	1940	0.25° x 0.25°	1-hourly
ECMWF UERRA-HARMONIE	UERRA	1	1961	11 km x 11 km	1-hourly

Table 3: Reanalysis data by 20CR and ECMWF used as forcing of the tide-surge model.

2.3 Tide-surge model

The water level simulations are done with the hydrodynamic tide-surge model TRIM- NP (Kapitza, 2008). TRIM is a Tidal, Residual and Intertidal Mudflat model and was originally developed by Casulli and Cattani (1994) and later nested and parallelised (-NP) by Kapitza (2008). Pätsch et al. (2017) tested and validated the model, also Gaslikova and Weisse (2013) used the model to simulate multi-decadal hydrodynamic conditions including hindcast and climate change projections (e.g., Gaslikova et al., 2013). Callies et al. (2011) used the TRIM-model data for drift simulations. Meyer et al., 2022 used this model to simulate the severe storm tides during the 1906 storm event.

All simulations are done in a barotropic mode within a 3-level nested set-up with regular Cartesian grids, having spatial resolutions from 12.6 km for the North-East Atlantic and the North Sea (grid 1), down to 1.6 km for the German Bight (grid 4), (Figure 3). The tides are calculated separately by FES2004 (Lyard et al., 2006) and introduced at the lateral boundaries of the coarsest grid. All model simulations started at least 15 days before each storm event and used zonal and meridional 10-meter height wind components and sea level pressure fields from the corresponding reanalysis as atmospheric forcing.

To explore the potential for the storm tide amplification for selected events, the historical tide was interchanged with a spring tide to simulate the highest physically possible water level depending on the respective weather situation during the event.
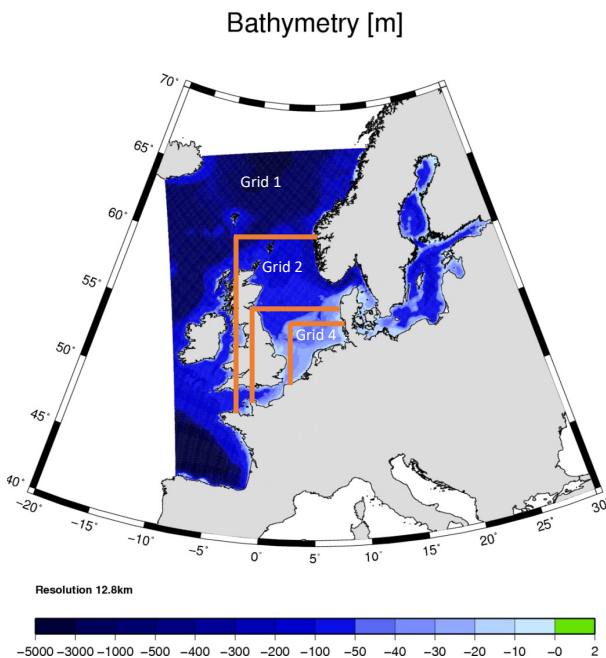
Figure 3: Trim model domain with grid 1 (12.8km resolution); grid 2 (6.4km), grid 3 (3.2km) and grid 4 (1.6km)

3 Results

3.1 Analysis of the storm tide event of 16 Feb 1962

On the example of one selected historical storm and a single location in the German Bight, we describe the temporal development of the storm and exemplarily the relations between different reanalyses and reanalysis members for both the storm tides and the underlying wind conditions. Figure 4 depicts the wind speeds near the Helgoland Island (Fig. 1) during 24 hours before and after the storm peak for the 1962 storm extracted from all used reanalyses as a representative of the marine atmospheric conditions in the German Bight. We do not use the observational wind data for comparison here because the wind measurements for Helgoland are somewhat impaired for certain wind conditions (Lindenberg et al.,2012) and it is not the topic of the present study to validate the reanalyses as that has been done extensively (Kristandt et al., 2014). During the 1962 storm, the wind speeds in the German Bight were not extremely high, but they exceeded 17.2 ms^{-1} (8Bft, Gale) for a long period. The

solid (coloured) lines represent ensemble members of 20CR reanalyses with the largest wind peak maximum. The grey lines show single members with a spread of about 7 ms^{-1} for the peak wind speeds for 20CRv3 (light grey) and about 3 ms^{-1} for 20CRv2c. The OptempS wind speeds, representing here the best guess wind conditions, are on the upper boundary of both sets of reanalyses. UERRA wind speeds, being very similar to OptempS in the temporal average, exhibit 6-hourly peaks. This is a known feature originating from the UERRA-specific 6-hourly re-forecasting procedure and was discussed by e.g. Schimanke et al. (2020) and Andrée et al. (2021). The peak of the ERA5 wind speed lags behind the peaks of other products and the wind speed is in general lower during the first half of the storm.
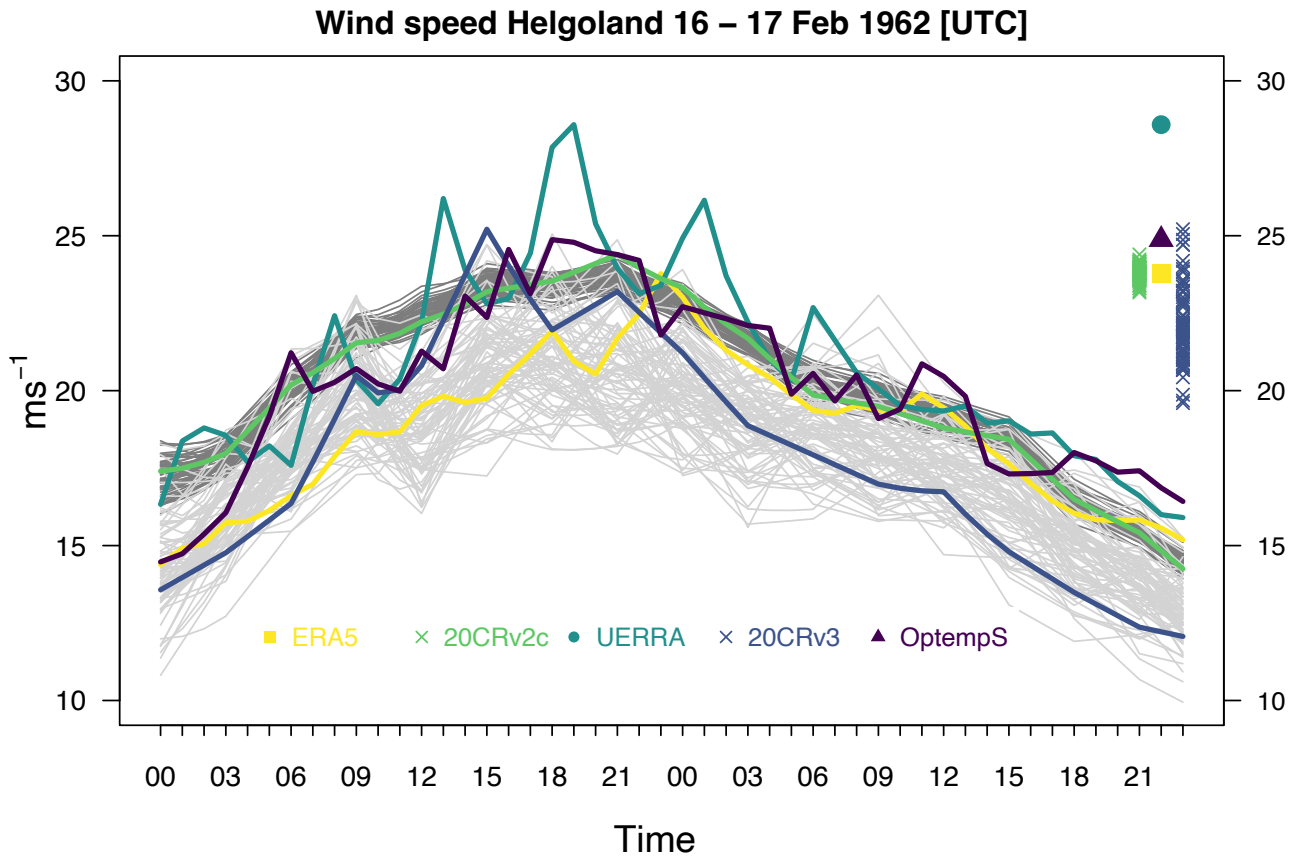

Figure 4: Wind speed near Helgoland for the event 16-17 Feb 1962 from UERRA in dark cyan, OptempS in dark violet, ERA5 in yellow, 20CRv2c (all ensemble members – dark grey, the member with the strongest wind – green) and 20CRv3 in light grey and blue for the highest member. On the right side, the highest peaks of the wind speed are shown for each reanalysis and each ensemble member.

The storm tides caused by the described atmospheric conditions are shown in Figure 5 for Cuxhaven, located in the Elbe estuary (Fig.1). In addition to the reanalyses, the tide gauge measurements at the location are depicted for comparison. The storm tide event continues for three tidal cycles. For the peak high water the observations lie well within the range of reanalyses ensemble. The range of the peak water levels from different reanalyses and reanalysis members is, however, rather high with about 1.5 m. Looking more into details, it can be inferred that results obtained with UERRA and OptempS forcings are very close to each other and slightly overestimate the observed peak high water. ERA5-driven storm tides underestimate the observed ones, which is consistent with the wind speed relation between ERA5 and UERRA/OptempS (Fig. 4). All 20CRv2c ensemble members overestimate observations and most of the other reanalyses, which agrees with the slightly higher 20CRv2c wind speeds during the first part of the storm (Fig. 4). Some of the ensemble members forced by the 20CRv3 are very close to

the observations, however the variability of the ensemble set is also large, following the variability of maximum wind speeds. We will follow the description of storm tide reanalyses for other storm events and locations using only the peak water levels from each realisation for comparison. For notions see an example on the right side of Figure 5.

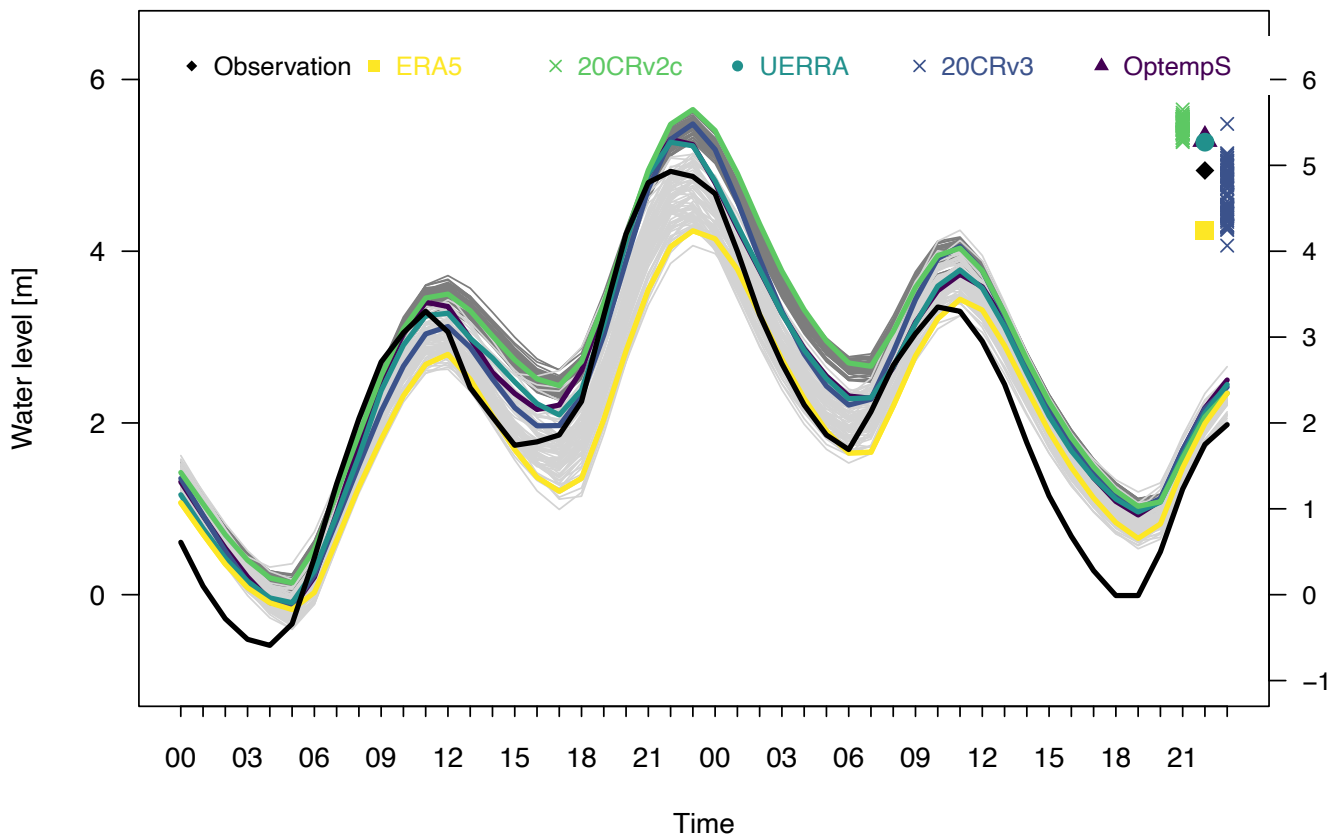## Cuxhaven, 16–17 Feb 1962

Figure 5: Observed and modelled water level for Cuxhaven for the event 16-17 Feb 1962. Observation is in black, simulated results are from model runs forced by various atmospheric reanalyses (see Fig. 4 for colour-coding).

### 3.2 Other storm tide events in the German Bight

To compare the effects of the eight investigated storms (see Table 2) on the water level at the different coastal stripes of the German Bight, we selected the following stations (Fig. 1): (a) Norderney (southern German Bight), (b) Cuxhaven (Elbe estuary) and (c) Husum (eastern German Bight). The tidal conditions are different for the three selected locations as the tidal wave travels counterclockwise in the North Sea, interacts with the relief and is formed by the combination of dissipation and reflection. In the German Bight, from east to west and from the open sea to the coast, there are several decimeter differences in the tidal range (Siefert and Lassen, 1996). Therefore, the tidal range at Norderney (2.46 m) is smaller than at Cuxhaven (2.94 m) and Husum (3.50 m), see also (Table A2). This, of course, affects the absolute water level heights during extreme events, but also the relative importance of the surge part for each storm tide.

Figure 6 shows storm tides from modelling results for the selected storm events at the three selected locations together with the corresponding observed maximum water levels. Additionally, for some events for which the potential for amplification was suspected, the results of additional experiments with tidal shift are shown. They represent the member of the 20CRv3 reconstruction which led to the highest storm tide and for which the water level simulation was repeated with the gradual temporal shift of spring tide instead of the historical tide. For the events with extreme surges that occurred during low tide, the observed low water is additionally depicted.

9

To discuss the results further, we subdivide the storm events according to the type of atmospheric situation they represent, as was described in Section 2.1. The multi-model ensemble exhibits similar behaviour within each type.

3.2.1 Scandinavia type

For the events of Scandinavia type, the storms of 1962, 21 Jan 1976 and 2013 with more northerly storm tracks (Fig. 2), the modelling results show, in general, a reasonable agreement with observations (Fig. 6). From the 20CRv3 ensemble, there are at least several members, which can reproduce historical hydrodynamic conditions for each event and at all three locations. The 20CRv2c ensemble displays less variability in peak water levels, although at least some members are still close to the observations, except for the 2013 event at Norderney and Cuxhaven (southern German Bight). This is consistent with a smaller variability of wind maxima for this ensemble compared to the next version 20CRv3 (see Fig. 4 and Fig. 8). UERRA and OptempS reconstructions also provide realistic atmospheric conditions for the simulation of extreme storm tides, resulting in estimations of water level maxima lying within 0.3 m (for 1962 and 21 Jan 1976 events) and 0.5 m (for 2013 event) range relative to observed values for all locations. Simulations driven by ERA5 atmospheric data generally underestimate the observed storm tides at all locations by several decimetres. This result could be anticipated from the wind conditions directly, with ERA5 winds typically having lower extreme wind speeds than e.g. UERRA or 20CRv3 during the selected storms (see e.g. Fig. 4 and Fig. 8). The Scandinavia type of storms often lead to large-scale storm surges, which affect the entire German Bight (e.g. Fig. 7a) leading to severe storm tides in all three selected locations and especially in the southern North Sea. In particular, during the storm of 1962, although water levels are slightly overestimated by UERRA and 20CRv2c reconstructions, at least four common members of the 20CRv3 ensemble could reproduce the observed extreme high water levels with the 10 cm accuracy at all three locations. This suggests the possibility of using the most fitting ensemble members for the reconstruction of the hydrodynamic conditions during this event for the entire coastline of the German Bight, covering with certain confidence even the coastal regions where the observational data were not available.
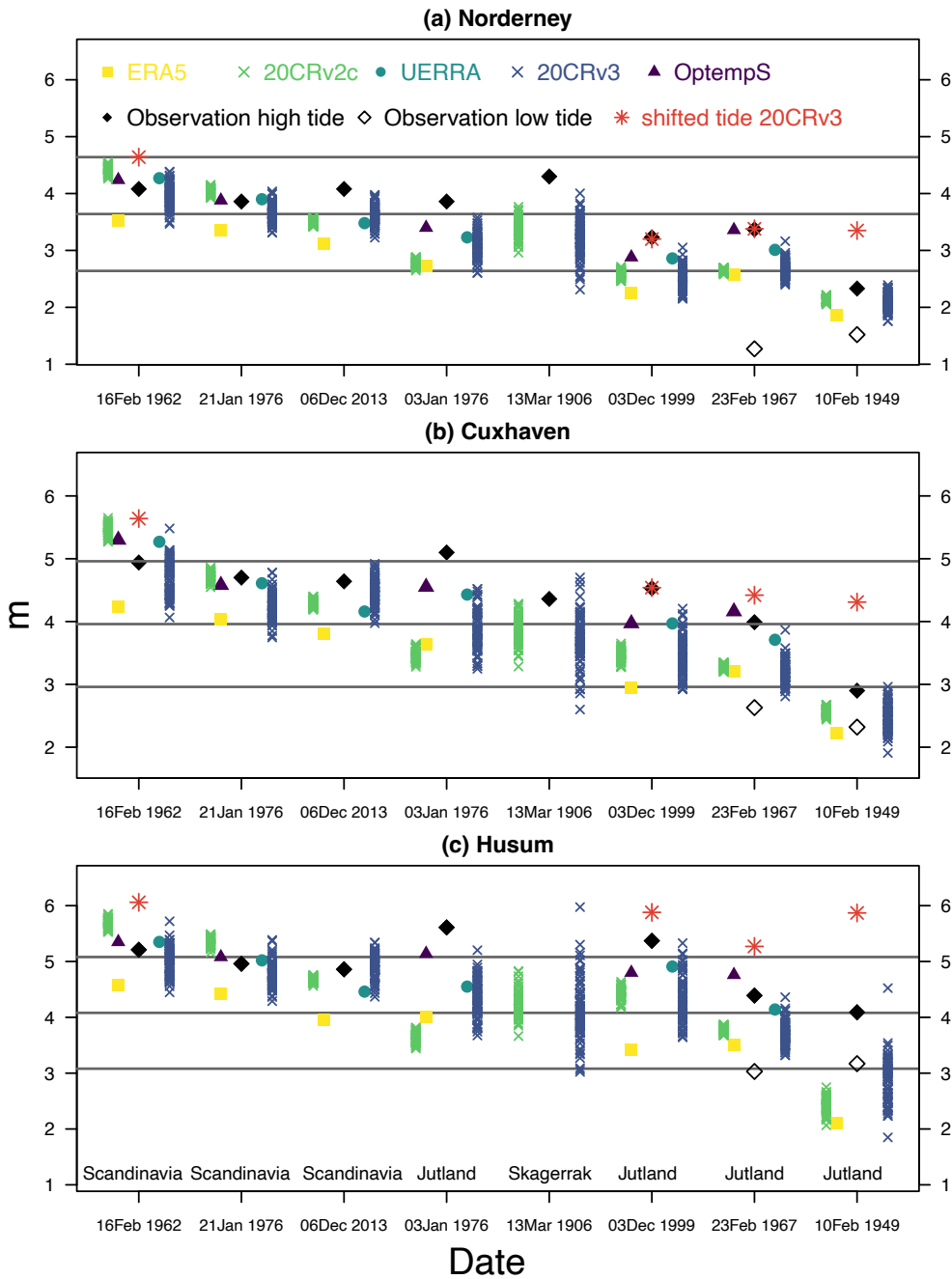
Figure 6: Maximum water levels in meter above normal Amsterdam level (Normaal Amsterdams Peil, NAP) for the three selected locations and the eight storm events. The different symbols and colours represent the different atmospheric forcing (see Table 2 and Fig. 4). The black diamonds stand for the observed water levels during high tide (filled) and low tide (unfilled). A red star marks the maximum water level from the tidal shift experiment for a selected member of the 20CRv3 reanalysis. The grey horizontal lines mark the level of very severe storm tide (top), severe storm tide (middle) and storm tide (bottom) for the respective locations (Table 1). The events are sorted according to the storm tracks crossing at 0° longitude and the types are defined crossing at 8° longitude.

3.2.2 Skagerrak type

Following the classification of storm tracks, the next type is Skagerrak (Figure A1) with storms moving along more south-located trajectories. One of the representatives of such storms was the event of 13 May 1906, responsible for one of the highest observed water levels in the southern German Bight. The detailed analysis of this storm event, issues with the reconstruction

11

of atmospheric conditions and the quality of the simulated storm tides can be found in Meyer et al., 2022. Here we show, for the sake of consistency, the ability of 20CR reanalysis to reproduce the storm consequences for Cuxhaven and Norderney. For Norderney, there were three reliable sources for observations available with the maximum water levels ranging from 3.84 to
300   4.30 m (Meyer et al., 2022). Depending on which observation source is considered more trustworthy, the peak water level is either slightly underestimated by all results of hydrodynamic modelling or selected ensemble members are able to reproduce the peak water level. For Cuxhaven, several members of hydrodynamic reanalysis show peak water levels close to the observed conditions.
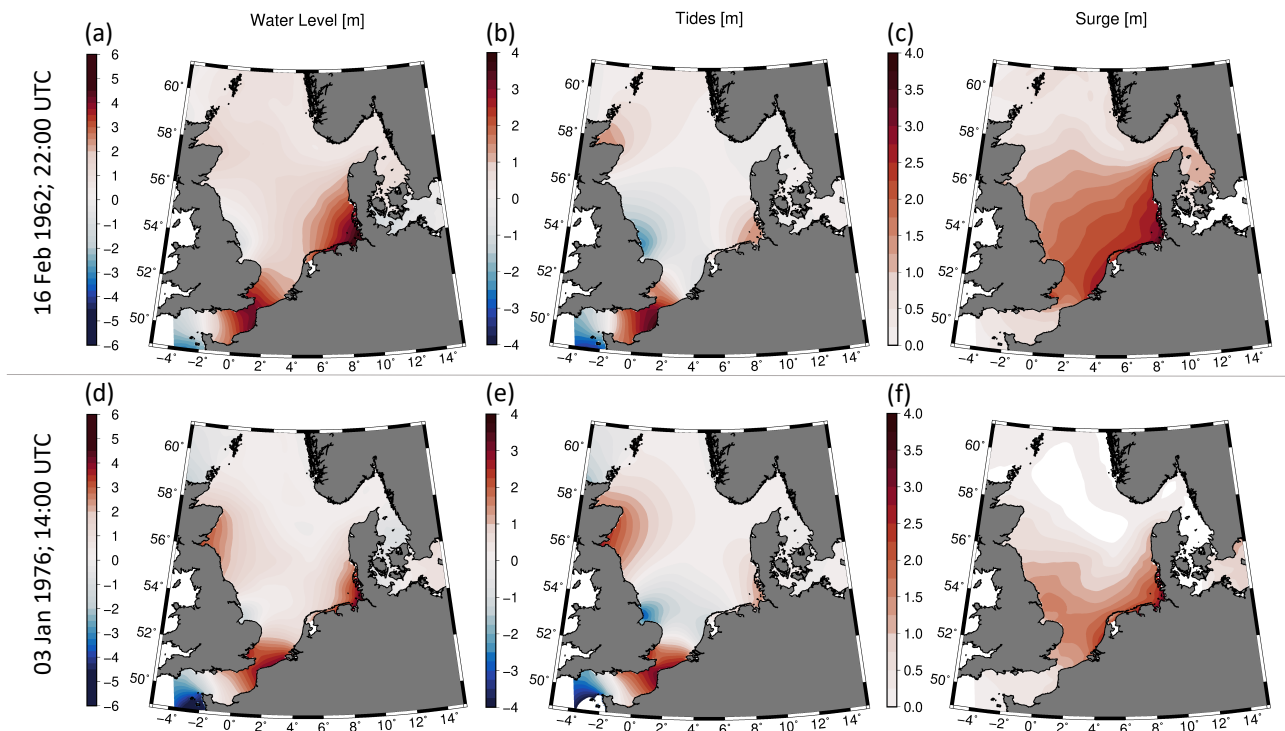
3.2.3 Jutland type

305   The representatives of the Jutland type of storms – 3 Jan 1976 and 3 Dec 1999 – are relatively fast storms moving through the North Sea almost from west to east (Fig. 2). With the cold front passing through the German Bight, they are characterised by shorter in time but more intensive wind speed extremes from south-westerly/westerly directions and rapid directional changes shortly before the storm peak in the German Bight (Fig. A4). This makes it more difficult for atmospheric reconstructions to capture and reproduce the particularities of the storm, which is reflected also in the results for peak water levels. All considered
310   reconstructions underestimate the peak water levels for both storms and all locations (Fig. 6, see also Table A5 for quantitative statistics). Although some members of the 20CRv3 reconstruction led to water levels close to the observed ones, the previous version 20CRv2c and ERA5 have difficulties to reproduce the exact historical storm conditions. It is assumed that, particularly for the storm on 3 Jan 1976, the atmospheric reconstructions may be lacking some short-term or small-scale meteorological phenomena crucial for the extreme storm surge formation.

315   ### 3.2.4 Differences in water level and surge between Scandinavia and Jutland type

To illustrate the effects of storm tracks on the spatial distribution of water levels in the North Sea, Figure 7 summarises the results for two storm events that exemplify the Scandinavian (16/17 February 1962, Figure 7a-c) and the Jutland type (3 January 1976, Figure 7d-f) of storm tracks. Both events caused the two highest observed water levels in Cuxhaven during the last century.
320   The panels show water level (Fig. 7a, 7d), tide (Fig. 7b, 7e) and surge as non-tidal residual (Fig. 7c, 7f) at the time of peak water level in Cuxhaven during the corresponding event as modelled using the merged atmospheric UERRA-OptempS forcing. The tidal component is estimated by model simulations without atmospheric forcing. Non-tidal residuals comprise (Fig. 7c,7f) wind surge and external surge but also consider inverse barometer effect and non-linear tide-surge interactions. In both situations, storm peaks approximately co-occurred with high tide in the German Bight (Fig. 7b, e). For the event in 1962, the
325   whole German Bight was affected by very high water and surge levels (Fig, 7a, c), whereas, during the event in 1976, only the east coast of the German Bight and the Elbe estuary experienced a very severe storm tide (Fig. 7d, f). Storm tracks of the Jutland type are moving much faster over the North Sea and have a shorter impact on the water level than the storms with northerly tracks. During the storm in 1962, additionally, a large contribution of external surge (Koopmann, 1962) raised the high surge in the entire southern North Sea. This phenomenon is mainly associated with the influence of low-pressure systems
330   in the North-East Atlantic via inverse barometer effect, then enhancement at the continental shelf and finally propagation into the North Sea (e.g., Böhme et al., 2023). Thus, the ability of atmospheric reconstructions to represent the intensity, location and speed of the low-pressure system in the North-East Atlantic also contributes to a more realistic representation of the storm tides in the German Bight.

Figure 7: Exemplary spatial distributions of water levels (a, d), tides (b, e) and surges (c, f) at the moment of maximum water level in Cuxhaven for the Scandinavia type storm (represented by the event of 16 Feb 1962, upper row) and the Jutland type storm (represented by the event 3 Jan 1976, lower row) modelled with the wind forcing by OptempS.

3.3 Variability and uncertainties due to atmospheric conditions

Taking advantage of the ensemble reconstructions, we look now at the effect of internal variability for each investigated storm event (Table 2). As a representative of atmospheric conditions in the German Bight, the wind speeds near Helgoland were selected. Figure 8 shows the maximum wind speeds for each considered storm obtained from each reanalysis or reanalysis member. There are several features of inter-reanalysis relations specific to different storms. For example, OptempS and UERRA wind maxima, showing always one of highest wind speeds among all reanalysis, are sometimes close to each other (e.g. for 3 Jan 1976 or 3 Dec 1999 storms) and for other events are different and exceeding all other reanalysis (e.g. 1962, 1967, 21 Jan 1976 storms). This can partly be attributed to somewhat artificial 6-hourly wind speed peaks in UERRA discussed for the 1962 storm example. These do not have a strong effect on the storm tide extremes, as can be seen for the 1962 and 21 Jan 1976 example storms in Figs. 5 and 6. Another distinction between the storms is the magnitude of 20CRv2c extremes relative to 20CRv3 extremes. Namely, they are sometimes at the upper range (e.g., for 1962), low range (e.g., 1967) or somewhere in between as for all other storms. These relations are not always transferable to the storm tide extremes, e.g., for the storm of 3 Jan 1976.
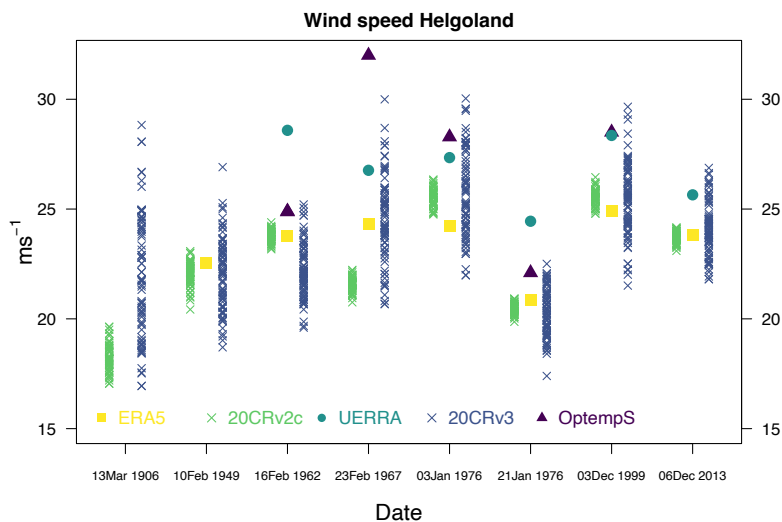
13

Figure 8: Maximum wind speed simulated by the reanalyses for the location Helgoland during each event. See also Table A3 and Figure A4.

There are also some features, which are common for all considered storm events. Such, the wind speed maxima from ERA5 reanalysis are generally lower than those from UERRA/OptempS and are within the range of the 20CRv3 ensemble. It is noticeable that the wind speeds from ERA5 are not higher than 25 ms^{-1} during these severe storm events. Haakenstad et al. (2021) and Dullaart et al. (2020) show, that ERA5 is underestimating very high wind speed compared to the observations. This is also reflected in the related storm tide extremes (Fig. 6), where extreme water levels forced by ERA5 lie at the lower range of other reanalysis and typically underestimate observations.

When we look at the spread of the wind maxima for different storms, the earlier storms, in particular 1906, show larger variability than more recent storms. This can be attributed to a smaller number of available observations for that period and thus less assimilated data, which leads to more degrees of freedom for the atmospheric circulation. In the year 1949, a large amount of data from the relevant regions had already been assimilated into the model for the Northern Hemisphere. Only surface pressure and wind data were used in the 20CR reanalysis, skipping the substantial increase in data available from satellites starting from 1980th.

This may increase the uncertainty of the 20CR reanalysis for the recent decades with respect to other datasets, however, it ensures the consistency of the data quality throughout the whole reanalysis period. This, in turn, enables us to notice the following differences in variability between the considered storms: it can be inferred (e.g. Fig. 8 and Table A3) that both 20CR ensembles demonstrate a larger uncertainty range of the maximum wind speed for the storms of Jutland type and notably smaller uncertainty for the Scandinavia type. As has been described earlier, during the Jutland-type storms the low-pressure area travels directly through the North Sea (e.g., Fig. A1) and the exact position and travel velocity of the low strongly influences the local wind speed and direction over the North Sea. Thus, the minor variations in the storm track or timing due to natural variability led to relatively large changes in the local wind speed maxima in the German Bight. Whereas for the Scandinavia type storms, with low-pressure areas travelling mostly beyond the North Sea, the wind is not that sensitive to the minor variations in the position and travel velocity of the low. It is also easier for other reanalysis with only one realisation to be more realistic in wind representation for the Scandinavia type, which makes it easier to reconstruct the storm tides realistically for these types of storms and it takes more effort to make it for the Jutland type, as is the case for the 3 Jan 1976 storm.

Another characteristic common for all storm events is a significantly smaller variability of the 20CRv2c ensemble with respect to 20CRv3 (Fig. 8 and Table A3). Whereas 20CRv2c wind speed maxima from different members are spread by 1.1 to 2.6 ms^{-1}

14

for a single location depending on the storm event, the 20CRv3 members are spread by 5.1 up to 11.9 ms^{-1}. The difference between 20CRv2c and 20CRv3 originates mainly in the different assimilation schemes and improved forecast systems by the National Centers for Environmental Prediction (NCEP) with higher resolution in both time and space (Slivinsky et al., 2019). The different uncertainty rates are also noticeable in the storm tide ensembles (Fig. 6, Table A5). For 20CRv2c, the peak storm tides spread between 0.15 m and 1m for various storm events with a median of 0.34 m. For 20CRv3, the spread increases to 0.95 - 2.1 m with a median of 1.16 m. These uncertainties are associated with the natural variability only, e.g., the slightly shifted location, timing or strength of atmospheric low-pressure system and consequent variability in high wind speed directions, duration and magnitude. Being physically consistent with the historical large-scale atmospheric conditions, these atmospheric realisations represent possible realistic developments of certain historic storms and thus realistic storm tides. It should be noted that some ensemble members of both 20CR reanalysis led to higher water levels than observed ones, hinting at potentially possible amplification of storm tides within the historical settings. This should be considered e.g., coastal protection design, which rests upon historic water level extreme among other criteria. Another point worth mentioning is that the ensemble mean values of maxima water levels underestimate the observed values almost for all events and both ensembles, with the exception of 1962 and 21 Jan 1976 storms simulated with 20CRv2c (Table A5). Whereas the selected ensemble members can reproduce or come close to the observed extreme water levels, especially for the Scandinavia type storms, the ensemble mean underestimation reaches up to 1.6m. Specifically for Jutland type events, the use of ensemble mean values for the representation of water level extremes is not recommended.

3.4 Amplification of storm tides by shifting tides

The storm events in 1949 and 1967, mentioned in Table 2 but not discussed so far, exhibited extreme atmospheric conditions but did not lead to extreme water levels at the coast. The event in 1967 was distinguished by exceptionally high wind speeds in the German Bight, the event in 1949 led to the highest recorded storm surge near Husum (Figures 6 and 8). During both events, the peak water levels were not noticeably high. The observed low waters at Husum, however, were the highest from the beginning of the record, indicating the presence of exceptionally high storm surges. Both events are reasonably represented, although slightly underestimated by at least some members of the water level reconstructions.

These two storm events represent examples of events which possibly could generate more severe peak water levels in case of a more unfortunate temporal coincidence of the storm peaks and high tide, especially spring high tide. To analyse the potential of these historical storm tides for amplification, physically consistent with the real conditions, additional numerical experiments were done. The member of the 20CRv3 ensemble which produced the highest storm tides during each event was selected to investigate whether these storm events could have caused much higher water levels at the coast under different tidal conditions. In the numerical experiments a spring tide and temporal shift of the tide were used together with the historical atmospheric conditions. It can be concluded, based on BSH categorisation for Norderney and Cuxhaven, that such storms would not result in very severe storm tides in any case, though the 1949 storm had more potential for an increase (about 1m for Norderney and about 1.35m for Cuxhaven). For Husum, if the event of 1949 would have happened under more unfavourable conditions, it would lead to very severe storm tides comparable to the historically observed maximum water level (Fig. 6). Such considerable amplification can be partly explained by larger tidal range near Husum and the funnel-shaped coastline, which exacerbate the changes by a switch from low tide to high spring tide. Additionally, being the Jutland type of storms, the 1949 and 1967 events caused a more pronounced surge at the eastern coast of the German Bight, affecting Husum at most of the selected three locations.

The possibility of higher water levels during different tidal conditions was also investigated for the events in 1962 and 1999. The ensemble members with the highest water level for 1962 and 1999 produced by 20CRv3 were shifted to a spring tide. In 1962, the simulated water level was already higher than the observed ones. This meets for all locations and presents the highest water level for all events: 4.64 m for Norderney; 5.64 m for Cuxhaven and 6.06 m for Husum. The water levels for the 1999

425   event were underestimated compared to the observed ones, but with the amplification of the tides, the water levels become higher, particularly in Husum.

4 Conclusion

We investigated some of the most prominent storm tides observed in the German Bight during the last 120 years. The water levels associated with the storms were simulated with a tide-surge model using atmospheric forcing from different reanalysis

430   products (20CR, ERA5 and UERRA). The resulting extreme storm tides were compared with observations for three locations at different coastal strips of the German Bight. The comparison of storm tide extremes with measurements gives a hint on the quality of the wind and pressure data and their capability to represent the atmospheric conditions during extreme storm events. In our investigation, we could show that the historical severe storm tides could be simulated realistically with individual members of 20CRv3, UERRA-HARMONIE as well as the merged UERRA-HARMONIE-OptempS reanalysis. Only the 03

435   Jan 1976 event could not be simulated satisfactorily using any of the considered reanalysis products and 1999 event was difficult to represent for the southern German Bight. The ERA5 data did not provide higher wind speed than 25 ms^{-1} close to the Helgoland location and all water level results are lower than the observed ones at the coast. Some differences between observed and modelled water levels were expected due to a range of factors not related to the atmospheric drivers. Such, the considered historical storm events occurred within the last 120 years, during which there were significant changes in

440   bathymetry, especially in the shallower areas and estuaries. Changes in the coastline due to erosion, consolidation and extensive protection constructions also took place. Additionally, the mean sea level rise is manifested in the region with changes of about 25cm during the period. All these changes were not accounted for in the present study. Additionally, there is a limitation due to the hydrodynamic model spatial resolution of 1.6 km and the ambiguity of some observational data, especially for older storms (e.g., 1906).

445   The maximum wind speeds during the storms showed more variability for the 20CRv3 ensemble than for 20CRv2c and the range encompassed the maxima winds from most of the other reconstructions. It translates also into the variability of storm tide peaks, leading to the differences from 0.95 m to 2.1 m between the 20CRv3 reconstruction members depending on the storm event. This uncertainty, representing the internal variability of the atmospheric system, indicates the realistic range of extreme storm tides associated with certain atmospheric situations. We have also considered an amplification mechanism due

450   to a combination of atmospheric and non-atmospheric conditions; in particular, we have shifted the tidal high water to coincide with the wind speed peak to get information on what is physically possible for the worst high water level at the coast. In these experiments, the extreme water levels would increase by a few decimetres. For the storm events 1949 and 1967 with shifted tides, the peak water levels would not be higher than the already observed ones in Norderney and Cuxhaven. For Husum, this experiment produced one of the highest observed or simulated water levels. This can be attributed mainly to the funnel-shaped

455   coastline and larger tidal range near the location but also storm surge distribution, which for these particular storms affected more the eastern than the southern parts of the German Bight. Shifting the tides to spring tide for the 1962 event resulted in the highest simulated water levels for all three locations. Generally, the shift of the tides shows a higher effect for the eastern German Bight than for the southern German Bight for the considered storms (Figure 6).

Furthermore, in our investigations we have distinguished between Scandinavia, Skagerrak, and Jutland type of storm tracks

460   over the North Sea and investigated their impact on the water levels at the German Bight coast. The northerly storm tracks cause a high surge over the entire southern North Sea. The southern storm tracks cause high surges on the eastern side of the German Bight (Figure 7). Generally, the water level in the German Bight can be simulated using reanalysis data, but the accuracy of reproducing the observed extreme water levels depends partly on the type of storm track. The simulated water levels in the German Bight coast are more uncertain and mostly underestimated compared to the observations when the storm

465   is categorised as Jutland type. One reason may be the incomplete reconstruction of the fast-running low over the southern
North Sea (Figure 2) in the forcing atmospheric data.

In summary, the various atmospheric reanalysis products are useful forcing data for investigating historical storm tides and
their effects on the coasts. The study of historical storm tides, on the other hand, may be considered for risk management in
case of coastal protection, which rests upon historical water level extremes among others.

470   However, there are still historical events that would benefit from further improvement of the atmospheric data with new
digitised historical pressure data, e.g., the severe storm in the Baltic Sea region in November 1872 (Feuchter et al., 2013;
Rosenhagen and Bork, 2009). Hawkins et al. (2023), for example, have shown that with new digitised historical pressure data
and an improved data assimilation process, the reanalysis of the severe windstorm over England and Wales in February 1903
could be significantly improved. Also, the simulations of the severe storm tides with a low-pressure area moving centrally

475   over the North Sea, like 03 Jan 1976 and 03 Dec 1999 events, need further improvements. These examples show that further
investigations and modelling efforts for severe windstorms and the resulting storm tides could be beneficial. This would
concern both the forecasting capability and thus the immediate risk awareness as well as the reconstruction potential and thus
the long-term planning of coastal protection and management.

480   **Appendix A**
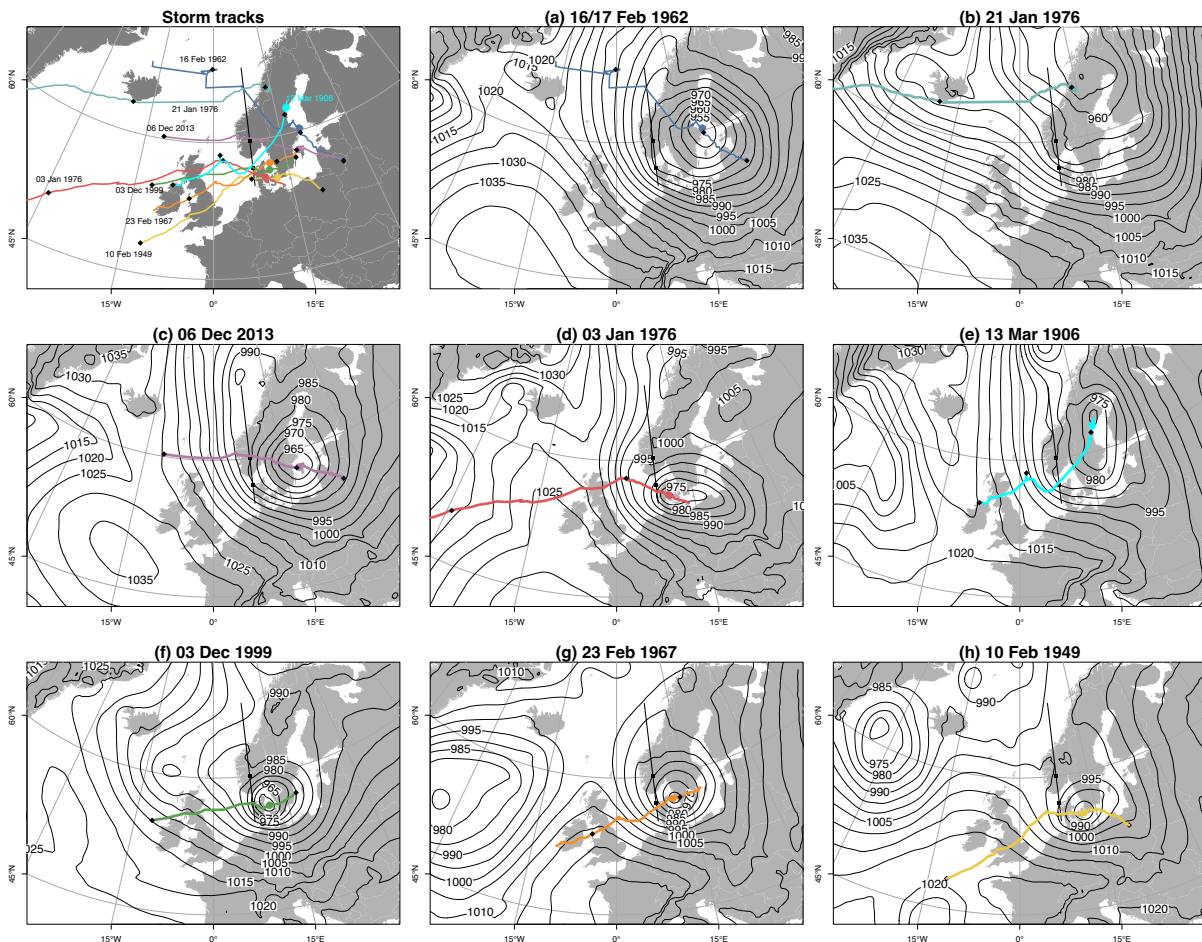
Figure A1: Storm tracks and mean sea-level pressure at the high peak of the storm are shown for the Scandinavia type (a-c),
485   Skagerrak type (e) and the Jutland type (d,f-h). The events are sorted according to the latitude of the storm tracks at longitude
0°. All tracks and mean sea-level pressure data are from ERA 5, only Figure (e) is calculated from 20CRv3. The tracks are
divided at 8° East into categories for the different types according to Prügel (1942), (black line).

17

	Norderney	Cuxhaven	Husum
	Long: 7.2° Lat:53.7°	Long: 8.7° Lat:53.9°	Long: 9.0° Lat: 54.5°
mean low water (MLW)	-1.23 m	-1.42 m	-1.80 m
mean high water (MHW)	1.23 m	1.52 m	1.70 m
tidal range	2.46 m	2.94 m	3.50 m

490

Table A2: Information about the locations of the tide gauge and their range, 10 years mean (2004-2013). (Deutsches Gewässerkundliches Jahrbuch, 2014)

	20CRv2c				20CRv3				OptempS
	Mini-mum	Median	Maxi-mum	STD	Mini-mum	Median	Maxi-mum	STD	Maximum
13 Mar 1906	17.04	18.21	19.65	0.64	16.94	21.79	28.83	2.84	--
10 Feb 1949	20.43	22.13	23.08	0.57	18.70	22.14	26.91	1.65	--
16 Feb 1962	23.17	23.81	24.40	0.26	19.60	22.12	25.21	1.24	24.87
23 Feb 1967	20.75	21.60	22.23	0.32	20.67	24.52	30.00	1.94	32.00
03 Jan 1976	24.75	25.56	26.34	0.40	21.98	25.31	30.03	1.92	28.44
21 Jan 1976	19.87	20.48	20.92	0.23	17.40	20.26	22.50	1.08	22.21
03 Dec 1999	24.79	25.51	26.45	0.37	21.51	25.5	29.66	1.67	28.51
06 Dec 2013	23.10	23.74	24.16	0.25	21.81	24.03	26.87	1.23	--

495   **Table A3:** Statistics of maximum wind speed of the ensembles during the severe storm event for the 20CRv2c and 20CRv3 products and OptempS for the location Helgoland (ms⁻¹).
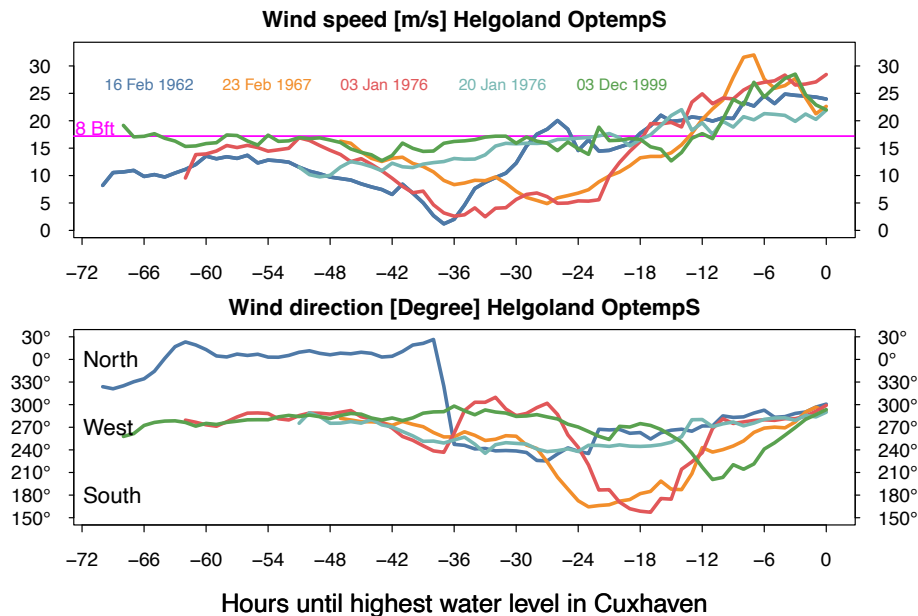
Figure A4: Wind speed and direction for the location Helgoland in hours before the highest water level in Cuxhaven. The
500   colours indicate the specific event. The light and dark blue colours indicate storms, which are categorised as Scandinavia type and the others are the Jutland type (orange, red, green).

18

Cuxhaven	20CRv2c				20CRv3			
	Max - Obs.	Mean - Obs.	Max - Min	STD	Max - Obs.	Mean - Obs.	Max - Min	STD
16 Feb 1962	0.71	0.52	0.38	0.09	0.54	-0.26	1.41	0.28
21 Jan 1976	0.16	0.02	0.31	0.07	0.08	-0.48	1.03	0.20
06 Dec 2013	-0.24	-0.35	0.21	0.05	0.28	-0.17	0.95	0.20
03 Jan 1976	-1.46	-1.63	0.36	0.09	-0.58	-1.23	1.27	0.30
03 Dec 1999	-0.88	-1.07	0.38	0.09	-0.32	-1.08	1.29	0.30
23 Feb 1967	-0.64	-0.70	0.15	0.04	-0.12	-0.79	1.06	0.18

Tab A5: Statistics of modelled water levels by 20CRv2c and by 20CRv3 and observation (Obs.) for the location Cuxhaven

505

Data availability

Video supplement

The animation of the reconstruction of the storm tide from 1906 is available on the TIB AV-Portal at
515 https://doi.org/10.5446/49529 (Meyer et al., 2020).

Author contribution

EM did the simulations and analysis. EM and LG have written the manuscript.

Competing interests

520 The authors declare that they have no conflict of interest.

Acknowledgements

References

Alexandersson, H., Schmith, T., Iden, K. and Tuomenvirta,H.: Long-term variations of the storm climate over NW Europe. Global Atmos. Ocean Syst., 6, 97–120. 1998.

Alexandersson, H., Tuomenvirta, H., Schmith, T. and Iden, K.: Trends of storms in NW Europe derived from an updated pressure data set. Climate Res., 14, 71–73. 2000

Andrée, E.; Su, J.; Larsen, M. A. D.; Madsen, K. S. & Drews, M. Simulating major storm surge events in a complex coastal region *Ocean Modelling, Elsevier BV*, 162, 101802. https://doi.org/10.1016/j.ocemod.2021.101802, 2021.

Arns, A., Wahl, T., Dangendorf, S., Jensen, J.: The impact of sea level rise on storm surge water levels in the northern part of the German Bight, Coastal Engineering, Volume 96, https://doi.org/10.1016/j.coastaleng.2014.12.002, 2015.

Arns, A., Wahl, T., Haigh, I.D., Jensen, J.: Determining return water levels at ungauged coastal sites: a case study for northern Germany. Ocean Dynamics **65**, 539–554. https://doi.org/10.1007/s10236-015-0814-1, 2015.

Böhme, A., Gerkensmeier, B., Bratz, B., Krautwald, C., Müller, O., Goseberg, N., and Gönnert, G.: Improvements to the detection and analysis of external surges in the North Sea, Nat. Hazards Earth Syst. Sci., 23, 1947–1966, https://doi.org/10.5194/nhess-23-1947-2023, 2023.

Bork, I.; Müller-Navarra, S.: Modellgestützte Untersuchungen zu Sturmfluten mit geringen Eintrittswahrscheinlichkeiten an der Deutschen Nordseeküste - Abschlussbericht Teil C - Sturmflutsimulation. Hg. v. Bundesamt für Seeschifffahrt und Hydrographie. 94 Seiten. https://doi.org/10.2314/GBV:514032537, 2006.

Casulli, V. and Cattani, E.: Stability, accuracy and efficiency of a semi-implicit method for three-dimensional shallow water flow, Comput. Math. Appl., 27, 99–112, 1994.

Callies, U., Plüß, A., Kappenberg, J., and Kapitza, H.: Particle tracking in the vicinity of Helgoland, North Sea: a model comparison, Ocean Dynam., 61, 2121–2139, https://doi.org/10.1007/s10236-011-0474-8, 2011.

Compo, G. P., Whitaker, J. S., Sardeshmukh, P. D., Matsui, N., Al- lan, R. J., Yin, X., Gleason, B. E., Vose, R. S., Rutledge, G., Bessemoulin, P., Brönnimann, S., Brunet, M., Crouthamel, R. I., Grant, A. N., Groisman, P. Y., Jones, P. D., Kruk, M., Kruger, A. C., Marshall, G. J., Maugeri, M., Mok, H. Y., Nordli, Ø., Ross, T. F., Trigo, R. M., Wang, X. L., Woodruff, S. D., and Worley, S. J.: The Twentieth Century Reanalysis Project, Q. J. Roy. Meteorol. Soc., 137, 1–28, https://doi.org/10.1002/qj.776, 2011.

Dee, D. P., Uppala, S. M., Simmons, A. J., Berrisford, P., Poli, P., Kobayashi, S., Andrae, U., Balmaseda, M. A., Balsamo, G., Bauer, P., Bechtold, P., Beljaars, A. C. M., van de Berg, L., Bidlot, J., Bormann, N., Delsol, C., Dragani, R., Fuentes, M., Geer, A. J., Haimberger, L., Healy, S. B., Hersbach, H., Hólm, E. V., Isaksen, L., Kållberg, P., Köhler, M., Matricardi, M., McNally, A. P., Monge-Sanz, B. M., Morcrette, J.-J., Park, B.-K., Peubey, C., de Rosnay, P., Tavolato, C., Thépaut, J.-N. and Vitart, F.: The ERA-Interim reanalysis: configuration and performance of the data assimilation system. Q.J.R. Meteorol. Soc., 137: 553–597. https://doi.org/10.1002/qj.828. 2011

Deutsches Gewässerkundliches Jahrbuch (DGJ): Küstengebiet der Nordsee 2013, Landesamt für Landwirtschaft, Umwelt und ländliche Räume Schleswig-Holstein Flintbek, ISSN 2193-6374, 2014.

Deutsches Institut für Normung e.V.: Hydrologie, Teil: 3 Begriffe zur quantitativen Hydrologie, Berlin, DIN 4049-3: 1994-10, Beuth Verlag GmbH, 10772 Berlin, 1994.

Dullaart, J.C.M., Muis, S., Bloemendaal, N. et al. Advancing global storm surge modelling using the new ERA5 climate reanalysis. Clim Dyn **54**, 1007–1021. https://doi.org/10.1007/s00382-019-05044-0. 2020

Feuchter, D., Jörg, C., Rosenhagen, G., Auchmann, R., Martius, O., and Brönnimann, S.: The 1872 Baltic Sea storm surge, in: Weather extremes during the past 140 years, edited by: Brönnimann, S. and Martius, O., Geographica Bernensia G89, 91–98, https://doi.org/10.4480/GB2013.G89.10, 2013.

Ganske, A., Fery, N., Gaskikova, L., Grabemann, I., Weisse, R. and Tinz, B.: Identification of extreme storm surges with high-impact potential along the German North Sea coastline. Ocean Dynamics,68, 1371–1382 https://doi.org/10.1007/s10236-018-1190-4, 2018.

Gerber, M., Ganske, A., Müller-Navarra, S., Rosenhagen, G.: Categorisation of Meteorological Conditions for Storm tide episodes in the German Bight. Meteorologische Zeitschrift, Vol. 25, No. 4, 447-462, 2016.

Gönnert, G: Sturmfluten und Windstau in der Deutschen Bucht - Charakter, Veränderungen und Maximalwerte im 20. Jahrhundert. Die Küste 67, 185-365, 2003.

Gönnert, G. and Gerkensmeier,B.: A Multi-Method Approach to Develop Extreme Storm Surge Events to Strengthen the Resilience of Highly Vulnerable Coastal Areas, Coastal Engineering Journal, 57:1, 1540002-1-1540002-26, https://doi.org/10.1142/S0578563415400021, 2015.

Gaslikova, L. and Weisse, R.: coastDat-2 TRIM-NP-2d Tide- Surge North Sea, World Data Center for Climate (WDCC) at DKRZ [data set], https://doi.org/10.1594/WDCC/coastDat- 2_TRIM-NP-2d, 2013.

Gaslikova L., I. Grabemann and N. Groll: Changes in North Sea storm surge conditions for four transient future climate realizations. Nat. Hazard, Vol 66, Issue 3, pp 1501-1518, doi: 10.1007/s11069-012-0279-1; 2013

Grabemann, I., L. Gaslikova, T. Brodhagen and E. Rudolph: Extreme storm tides in the German Bight (North Sea) and their potential for amplification. Nat. Hazards Earth Syst. Sci., 20, pp 1–16, https://doi.org/10.5194/nhess-20-1-2020, 2020

Haakenstad, H., Breivik, Ø., Furevik, B. R. Reistad, M., Bohlinger,P. and Aarnes, O. J.: NORA3: A Nonhydrostatic High-Resolution Hindcast of the North Sea, the Norwegian Sea, and the Barents Sea. J. Appl. Meteor. Climatol., **60**, 1443–1464, https://doi.org/10.1175/JAMC-D-21-0029.1. 2021.

Hawkins, E., Brohan, P., Burgess, S. N., Burt, S., Compo, G. P., Gray, S. L., Haigh, I. D., Hersbach, H., Kuijjer, K., Martínez-Alvarado, O., McColl, C., Schurer, A. P., Slivinski, L., and Williams, J.: Rescuing historical weather observations improves

quantification of severe windstorm risks, Nat. Hazards Earth Syst. Sci., 23, 1465–1482, https://doi.org/10.5194/nhess-23-1465-2023, 2023.

595 Hersbach, H., Bell, B., Berrisford, P., Biavati, G., Horányi, A., Muñoz Sabater, J., Nicolas, J., Peubey, C., Radu, R., Rozum, I., Schepers, D., Simmons, A., Soci, C., Dee, D., Thépaut, J-N. (2018): ERA5 hourly data on single levels from 1940 to present. Copernicus Climate Change Service (C3S) Climate Data Store (CDS). 10.24381/cds.adbb2d47 , (Accessed on 01-APR-2023)

Hersbach, H., Bell, B., Berrisford, P., Hirahara, S., Horányi, A., Muñoz-Sabater, J., Nicolas, J., Peubey, C., Radu, R., Schepers, D., Simmons, A., Soci, C., Abdalla, S., Abellan, X., Balsamo, G., Bechtold, P., Biavati, G., Bidlot, J., Bonavita, M., De
600 Chiara, G., Dahlgren, P., Dee, D., Diamantakis, M., Dragani, R., Flemming, J., Forbes, R., Fuentes, M., Geer, A., Haimberger, L., Healy, S., Hogan, R. J., Hólm, E. Janisková, M., Keeley, S., Laloyaux, P., Lopez, P., Lupu, C., Radnoti, G., de Rosnay, P., Rozum, I., Vamborg, F., Villaume, S., Thépaut, J.-N.: The ERA5 global reanalysis. *Q J R Meteorol Soc*. 2020; 146: 1999–2049. https://doi.org/10.1002/qj.3803. 2020

Horsburgh, K. J. and Wilson, C.: Tide-surge interaction and its role in the distribution of surge residuals in the North Sea, J.
605 Geophys. Res., 112, C08003, https://doi.org/10.1029/2006JC004033, 2007.

Jensen, Jürgen; Mudersbach, Christoph; Müller-Navarra, Sylvin H.; Bork, Ingrid; Koziar, Christian; Renner, Volker: Modellgestützte Untersuchungen zu Sturmfluten mit sehr geringen Eintrittswahrscheinlichkeiten an der deutschen Nordseeküste. Hg. v. Kuratorium für Forschung im Küsteningenieurwesen (Die Küste, 71). 2006

Kristandt,J., Brecht,B., Frank, H. and Knaack, H.: Optimization of Empirical Storm Surge Forecast - Modelling of High
610 Resolution Wind Fields. Hg. v. Kuratorium für Forschung im Küsteningenieurwesen (Die Küste, 81). Seite 301- 318, 2014.

Kapitza, H.: MOPS – A Morphodynamical Prediction System on Cluster Computers, in: High performance computing for computational science-VECPAR 2008, edited by: Laginha, J. M., Palma, M., Amestoy, P. R., Dayde, M., Mattoso, M., and Lopez, J., Lecture Notes in Computer Science, Springer, pp. 63–68, https://doi.org/10.1007/978-3-540-92859-1_8,
615 2008.

Koopmann, G.: Die Sturmflut vom 16./17. Februar 1962 in ozeanographischer Sicht. Die Küste 10/2, 55–68, 1962.

Kruhl, H.: Sturmflutwetterlagen, – Promet **8**(4), 6–8. 1978.

Kuratorium für Forschung im Küsteningenieurwesen: Die Küste, 33 Sturmfluten 1976. Archiv für Forschung und Technik an der Nord- und Ostsee. Archive for Research and Technology on the North Sea and Baltic Coast.
620 https://hdl.handle.net/20.500.11970/101135. 1979.

Lamb, H.: Historic storms of the North Sea, British Isles and Northwest Europe. Cambridge University Press, 2005

Lindenberg, J.; Mengelkamp, H.-T.; Rosenhagen, G.: Representativity of near surface wind measurements from coastal stations at the German Bight. In: Meteorologische Zeitschrift. Vol. 21, 2012. DOI: 10.1127/0941-2948/2012/0131

Lyard, F., Lefèvre, F., Letellier, T., and Francis, O.: Modelling the global ocean tides: a modern insight from FES2004,
625 Ocean Dynamics., 56, 394–415, https://doi.org/10.1007/s10236-006-0086-x, 2006.

Meyer, E. M. I., Weisse, R., Grabemann, I., Tinz, B., and Scholz, R.: Reconstruction of wind and surge of the 1906 storm tide at the German North Sea coast, Nat. Hazards Earth Syst. Sci., 22, 2419–2432, https://doi.org/10.5194/nhess-22-2419-2022, 2022.

Meyer, E., Weisse, R., and Böttinger, M.: The storm tide in March 1906, TIB [video supplement],
630 https://doi.org/10.5446/49529, 2020.

Meyer, E.: Reconstruction of the 1906 Storm Tide in the German Bright using TRIM-NP, FES2004, and NOAA-CIRES-DOE Twentieth Century Reanalysis (20CR) version 2c and 3, World Data Center for Climate (WDCC) at DKRZ [data set], https://doi.org/10.26050/WDCC/storm_tide_1906_20CR, 2021.

Meyer, Elke M. I.: coastDat historical severe storm tides in the German Bight. World Data Center for Climate (WDCC) at
635 DKRZ. https://doi.org/10.26050/WDCC/CoastdatStormTides. 2023.

Oumeraci, H., Kortenhaus, A., Burzel, A., Naulin, M., Dassanayake, D. R., Jensen, J., Wahl, T., Mudersbach, C., Gönnert, G., Gerkensmeier, B., Fröhle, P., and Ujeyl, G.: XtremRisK – Integrated Flood Risk Analysis for Extreme Storm Surges at Open Coasts and in Estuaries: Methodology, Key Results and Lessons Learned, Coast. Eng. J., 57, 1540001-1–1540001-23, https://doi.org/10.1142/S057856341540001X, 2015.

640 Pätsch, J., Burchard, H., Dieterich, C., Gräwe, U., Gröger, M., Mathis, M., Kapitza, H., Bersch, M., Moll, A., Pohlmann, T., Su, J., Ho-Hagemann, H. T. M., Schulz, A., Elizalde, A., and Eden, C.: An evaluation of the North Sea circulation in global and regional models relevant for ecosystem simulations, Ocean Model., 116, 70–95, https://doi.org/10.1016/j.ocemod.2017.06.005, 2017.

Petersen, M. and Rhode, H.: Sturmflut. Die großen Fluten an den Küsten Schleswig-Holsteins und in der Elbe. Karl
645 Wachholtz Verlag, Neumünster, 1991.

Prügel, H. : Die Sturmflutschäden an der schleswig-holsteinischen Westküste in ihrer meteorologischen und morphologischen Abhängigkeit. Schriften des Geographischen Instituts der Universität Kiel, Band XI, Heft 3. Dietrich Reimer, Andrews & Stiner, Berlin, 1942.

Ridal, M., Schimanke, S., and Hopsch, S.: Documentation of the RRA system:
650 UERRA. Ref.:C3S_D322_Lot1.1.1.2_201802_Documentation_of_UERRA_v2.2018

Rodewald, M.: Zur Entstehungsgeschichte der Sturmflut-Wetterlagen in der Nordsee im Februar 1962. In: Die Küste 10, 2. Heide, Holstein: Boyens. S. 1-54, 1962.

Rosenhagen, G. and Bork, I.: Rekonstruktion der Sturmflutwetterlage vom 13. November 1872, Die Küste, 75, MUSTOK, 51–70, 2009.

655   Schelling, H.: Die Sturmfluten an der Westküste von Schleswig-Holstein unter besonderer Berücksichtigung der Verhältnisse am Pegel Husum. In: Die Küste 1, 1. Heide, Holstein: Boyens. S. 63-146. https://hdl.handle.net/20.500.11970/100568; 1952.

Schimanke, S., Isaksson, L., Edvinsson, L., Undén, P., Ridal, M., Moigne, P., Bazile, E., Verrelle, A., Glinton, M., 2020. UERRA Data User Guide. ECMWF Copernicus Note, Swedish Meteorological and Hydrological Institute (SMHI),
660   version 3.3. URL: http://datastore.copernicus-climate.eu/documents/uerra/D322_Lot1.4.1. 2_User_guides_v3.3.pdf. (Accessed 03 August 2023).

Schmidt, H., von Storch, H. German Bight storms analysed. Nature 365, 791. https://doi.org/10.1038/365791a0; 1993

Siefert, W.; Lassen, H.: Tideablauf und Meeresspiegel im Bereich der südöstlichen Nordsee-Amphidromien. In: Die Küste 58. Heide, Holstein: Boyens. S. 109-160. https://hdl.handle.net/20.500.11970/101389. 1996.

665   Slivinski, L. C., Compo, G. P., Whitaker, J. S., Sardeshmukh, P. D., Giese, B. S., McColl, C., Allan, R., Yin, X., Vose, R., Titchner, H., Kennedy, J., Spencer, L. J., Ashcroft, L., Brönnimann, S., Brunet, M., Camuffo, D., Cornes, R., Cram, T. A., Crouthamel, R., Domínguez-Castro, F., Freeman, J. E., Gergis, J., Hawkins, E., Jones, P. D., Jourdain, S., Kaplan, A., Kubota, H., Le Blancq, F., Lee, T.-C., Lorrey, A., Luterbacher, J., Maugeri, M., Mock, C. J., Moore, G. W. K., Przybylak, R., Pudmenzky, C., Reason, C., Slonosky, V. C., Smith, C. A., Tinz, B., Trewin, B., Valente, M. A., Wang, X. L., Wilkinson,
670   C., Wood, K., and Wyszynski, P.: Towards a more reliable historical re- analysis: Improvements for version 3 of the Twentieth Century Reanalysis system, Q. J. Roy. Meteorol. Soc., 145, 2876–2908, https://doi.org/10.1002/qj.3598, 2019.

Slivinski, L. C., Compo, G. P., Sardeshmukh, P. D., Whitaker, J. S., McColl, C., Allan, R., Brohan, P., Yin, X., Smith, C.A., Spencer, L.J., Vose, R.J., Rohrer, M., Conroy, R.P., Schuster, D. C., Kennedy, J. J., Ashcroft, L., Brönnimann, S., Brunet, M., Camuffo, D., Cornes, R., Cram, T. A., Domínguez-Castro, F., Freeman, J. E., Gergis, J., Hawkins, E., Jones, P. D., H.
675   Kubota, H., Lee, T. C., Lorrey, A. M., Luterbacher, J., Mock, C. J., Przybylak, R.K., Pudmenzky, C., Slonosky, V.C., Tinz, B., Trewin, B., Wang, X. L., Wilkinson, C., Wood, K., and Wyszyński, P.: An Evaluation of the Performance of the Twentieth Century Reanalysis Version 3. J. Climate, 34, 1417–1438, https://doi.org/10.1175/JCLI-D-20-0505.1. 2021

Streicher, M., Kristandt, J., and Knaack, H.: Optimierung Empirischer Sturmflutvorhersagen (OptempS-MohoWif A), Niedersäsischer Landesbetrieb für Wasserwirtschaft, Küsten- und Naturschutz (NLWKN), 2015.
680   Tomczak, G.: Die Sturmfluten vom 9. Und 10. Februar 1949 an der deutschen Nordseeküste. Deutsche Hydrographische Zeitschrift 3, 227–240 (1950). https://doi.org/10.1007/BF02026795, 1950.

UERRA: Complete UERRA regional reanalysis for Europe from 1961 to 2019. https://doi.org:10.24381/cds.dd7c6d66

Uppala, S.M., KÅllberg, P.W., Simmons, A.J., Andrae, U., Bechtold, V.D.C., Fiorino, M., Gibson, J.K., Haseler, J., Hernandez, A., Kelly, G.A., Li, X., Onogi, K., Saarinen, S., Sokka, N., Allan, R.P., Andersson, E., Arpe, K., Balmaseda,
685   M.A., Beljaars, A.C.M., Berg, L.V.D., Bidlot, J., Bormann, N., Caires, S., Chevallier, F., Dethof, A., Dragosavac, M., Fisher, M., Fuentes, M., Hagemann, S., Hólm, E., Hoskins, B.J., Isaksen, L., Janssen, P.A.E.M., Jenne, R., Mcnally, A.P., Mahfouf, J.-F., Morcrette, J.-J., Rayner, N.A., Saunders, R.W., Simon, P., Sterl, A., Trenberth, K.E., Untch, A., Vasiljevic, D., Viterbo, P. and Woollen, J.: The ERA-40 re-analysis. Q.J.R. Meteorol. Soc., 131: 2961-3012. https://doi.org/10.1256/qj.04.176, 2005.
690   van Bebber, W. J.: Bemerkenswerte Stürme, Annalen der Hydrographie und maritimen Meteorologie: Zeitschr. für Seefahrt u. Meereskunde/Deutsche Seewarte in Hamburg, ISSN 0174-8114, OCLC-Nr. 183317596, 1906.

Vousdoukas, M.I., Voukouvalas, E., Annunziato, A., Giardino A. and Feyen, L.: Projections of extreme storm surge levels along Europe. Clim Dyn 47, 3171–3190. https://doi.org/10.1007/s00382-016-3019-5, 2016.

Weisse, R. and Plüß, A.: Storm-related sea level variations along the North Sea coast as simulated by a high-resolution model
695   1958-2002. Ocean Dynamics, 56, 16-25, https://doi.org/10.1007/s10236-005-0037-y, 2006.

Weisse, R., Bisling, P., Gaslikova, L., Geyer, B., Groll, N., Hortamani, M., Matthias, V., Maneke, M., Meinke, I., Meyer, E.M.I., Schwichtenberg, F., Stempinski, F., Wiese, F. and Wöckner-Kluwe, K.,: Climate services for marine applications in Europe. Earth Perspectives 2, 3, https://doi.org/10.1186/s40322-015-0029-0, 2015.

700